J Mater Sci (2007) 42:9783–9794
DOI 10.1007/s10853-007-1984-0

Generation of phosphor particles for photoluminescence applications by spray pyrolysis

Sukwon Jung · Yun Chan Kang · Jung Hyeun Kim

Received: 4 April 2007 / Accepted: 9 July 2007 / Published online: 11 August 2007

Abstract Phosphor materials have been used for applications in fluorescence lamps and display devices. Such phosphors have been mostly produced by the conventional solid-state reaction technique. In solid-state reactions, high reaction temperature and long heating time are required to obtain a pure phase of the multi-component particles, and agglomerated particles of irregular shape is unavoidable. Therefore, milling process is necessary in the solid-state technique. These process characteristics decrease the brightness of phosphor particles. Recently, extensive efforts were given in production of phosphors particles by spray pyrolysis in order to have fine size and spherical morphology. In this manuscript, phosphor particles produced by spray pyrolysis for photoluminescence applications were reviewed. Phosphorescence phenomenon is briefly explained with the energy transfer mechanism including the intersystem crossing. In the main context, phosphor materials are categorized into three parts following the color (red, green, and blue) characteristics. As expected, phosphor particles generated by spray pyrolysis have a big advantage in obtaining spherical morphology, compared with the particles from the conventional solid-state processes. Therefore, high packing density and uniformity of films for final display devices are predicted, and it could further help achieving high photoluminescent intensity in final products.

S. Jung · J. H. Kim (✉)
Department of Chemical Engineering, University of Seoul, Seoul 130-734, Korea
e-mail: jhkimad@uos.ac.kr

Y. C. Kang
Department of Chemical Engineering, Konkuk University, Seoul 143-701, Korea

Introduction

Phosphor materials are generally composed of a pure host matrix and a small amount of intentionally added impurity, so-called activator [1]. If the host material and the activator concentrations are fixed, the physical properties of phosphor materials such as the surface area, the crystallinity, the phase purity, and the distribution of activator in the host matrix play crucial roles in modulating luminescence characteristics. Those material properties can be controlled by the preparation conditions: temperature, precursor concentration, gas flow rate, and post annealing. Especially, the preparation and annealing temperatures greatly influence the luminescence intensity of phosphor particles since it directly affects the formation of crystal structure, crystallinity, the surface area of particles, and the distribution of activator.

The conventional solid-state reaction is mainly used to prepare phosphor particles, but it has a big disadvantage in controlling particle morphology. On the other hand, spray pyrolysis is attracting because it is easy to produce spherical and non-aggregate particles. Recently, extensive efforts on the generation of phosphor particles by spray pyrolysis have been given with increasing attention of their applications to a plasma display panel (PDP) and a fluorescent lamp. Spray pyrolysis is widely used in generation of spherical micro- or nano-scale particle materials. Figure 1 shows a general scheme for production of phosphor particles by spray pyrolysis. For phosphor particles, two furnaces in series are necessary to enhance crystallinity of materials. The first furnace helps formation of primary particles, and the second furnace further increases material crystallization. It is a relatively simple method to produce large amount of particles in a continuous manner as long as there are a high temperature furnace reactor, a carrier gas, and a precursor. In addition, particle morphology formed

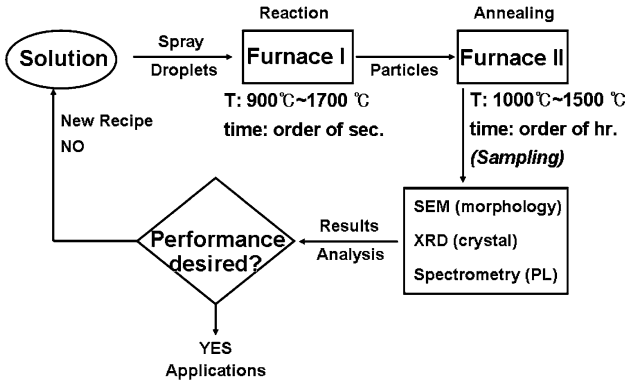

Fig. 1 General scheme for development of phosphor particles by spray pyrolysis

by the spray pyrolysis is highly spherical, and thus it increases the packaging density and surface uniformity to apply for the flat panel display devices. Photoluminescence (PL) intensity can be increased with those advantages from the particles produced by the spray pyrolysis.

Although spray pyrolysis has a number of advantages, it is also challenging because hollow and highly porous particles are formed. The hollow particles have low thermal stability, and the porosity of hollow particles is increased by post-treatment for the crystallization and activation of phosphor particles. Especially, when the concentration of the precursor salt is increased for high productivity, hollow particles are easily generated. These structural defects can lead to reduced luminescent characteristics. To decrease those defects of phosphor particles, some additive components can be added. Flux materials, colloidal seeds, organic compounds are considered for the conventional spray pyrolysis process. In addition, flame spray pyrolysis is also considered as a potential process for the preparation of dense particles.

In this article, various materials produced by spray pyrolysis for red, green, blue phosphors were extensively reviewed depending on the combinations of matrix and activator compositions. The basic principle of phosphorescence is briefly explained in next section to help understanding photoluminescence phenomena. In the following main context, numerous studies to improve particle morphology and the PL intensity of phosphor particles were reviewed. Materials reviewed are: Y_2O_3:Eu, Gd_2O_3:Eu, $(Y,Gd)_2O_3$:Eu, $(Y,Gd)BO_3$:Eu, YAG:Eu, YVO_4:Eu, ZrO_2:Eu, SiO_2:Eu, $(Y,Gd)Al_3(BO_3)_4$:Eu, $SrTiO_3$:(Pr,Al), $CaTiO_3$:Pr, $Y(P,V)O_4$:Eu for red ; Zn_2SiO_4:Mn, $(Ce,Tb)MgAl_{11}O_{19}$, Y_2SiO_5:Tb, YAG:Ce, YAG:Tb, $BaAl_{12}O_{19}$:Mn, $GdPO_4$:Tb, $LaPO_4$:(Tb,Mn), $ZnGa_2O_4$:Mn, YBO_3:Tb, $LaPO_4$:(Ce,Tb), $(Ba,Sr)_2SiO_4$:Eu, YVO_4:Dy, $Ca_8Mg(SiO_4)_4Cl_2$:Eu, (Sr,Zn) Al_2O_4:(Eu,B) for green; $BaMgAl_{10}O_{17}$:Eu, Sr_2CeO_4, $Sr_5(PO_4)_3Cl$:Eu, Y_2SiO_5:Ce, $CaMgSi_2O_6$:Eu for blue.

Phosphorescence

The word *luminescence* includes both *fluorescence* and *phosphorescence* [1]. The *luminescence* is defined as a phenomenon in which the electronic state of a substance is excited by some kind of external energy and the excitation energy is given off as light. Here, the word light includes not only electromagnetic waves in the visible region of 400 to 700 nm, but also those in the neighboring regions on both ends, i.e., the near-ultraviolet and the near-infrared regions. In modern usage, light emission from a substance during the time when it is exposed to exciting radiation is called *fluorescence*, while the after-glow if detectable by the human eye after the cessation of excitation is called *phosphorescence*. Generally, the timescale for photon emission for *phosphorescence* (on the order of 10^{-4} to 10^{+4} s) is slower than for *fluorescence* (on the order of 10^{-10} to 10^{-6} s) [2]. The definition of phosphor itself is not clearly defined and is dependent on the user. In a broader sense, the word phosphor is equivalent to "solid luminescent material."

The light emission depends on material structure and morphology, basically atomic interaction associated with luminescence center and the host lattice material [3]. Phosphor materials consist of the host matrix and the activator, and the activator is the luminescent center in the host with a small amount of rare-earth metallic impurities, as shown in Fig. 2a. When the excitation sources such as ultraviolet (UV) or vacuum-UV (VUV) lights hit the phosphor particles, they experience a phosphorescence process: absorption, excitation, relaxation, and emission, as depicted in Fig. 2b. The light is absorbed by the host material, and the absorbed energy is transferred from the host to the activator. Finally, the activator emits visible light through the energy transfer mechanism. Figure 2c shows the schematic representation of the energy transfer mechanism, and it is well described in physical chemistry textbooks [2, 4]. The singlet ground state (S_0) of the activator energy level is excited to the singlet-excited state (higher than S_1) by absorbing energy from the host. After the absorption, the initial excited states undergo radiationless transition by giving up energy to the surroundings. The importance step in phosphorescence is the intersystem crossing, the switch from a singlet state (S_1) to a triplet state (higher than T_1) brought about by spin-orbit coupling. In a triplet state, it is now stepping down the triplet's vibrational ladder, and at the lowest energy level it is trapped because the triplet state (T_1) is at a lower energy than the corresponding singlet (S_1). The triplet state (T_1) acts as a slowly radiating reservoir because the return to the ground state (S_0) is spin-forbidden.

In the phosphorescence process, color is determined by materials used. For example, under VUV as an excitation

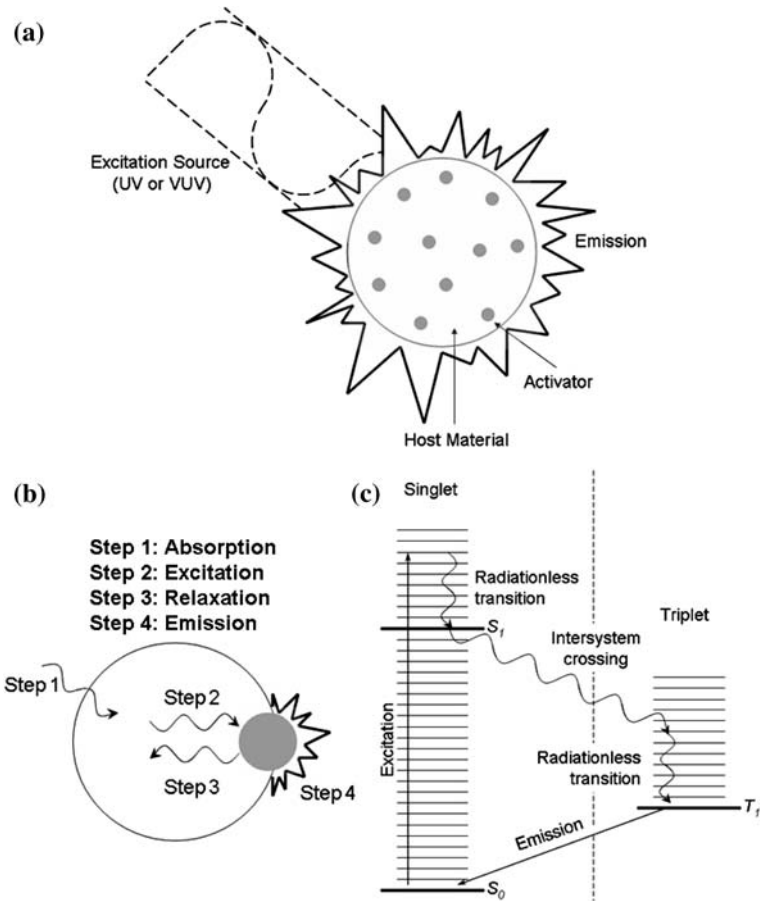

Fig. 2 Schematic representation of the light emission process from the phosphor particles. UV or VUV is used as excitation sources shown in (**a**). The light is absorbed by the host material, the energy is transferred from the host to the activator, and finally it emits visible light as shown in (**b**). The energy transfer mechanism for phosphorescence is shown in (**c**)

source, (Y,Gd)BO_3:Eu or Y_2O_3:Eu (red), Zn_2SiO_4:Mn (green), and $BaMgAl_{10}O_{17}$:Eu (blue) are representative phosphor materials. Generally, the most of the light emitting devices utilizes red, green, and blue colors for practical applications. Therefore, in this manuscript we are classifying the phosphors into three categories for red, green, blue color materials.

Red phosphor

Y_2O_3:Eu

It is the most popular phosphor material in the red color applications for display devices. Based on the many published articles for this theme, crystallinity and particle morphology play a major role in enhancing photoluminescence (PL) intensity. In addition, particle size distribution, crystal structure, particle aggregation, and impurity contents can also change the PL intensity. In crystallinity point of view, the higher crystallization can be achieved either by increasing reaction temperature and residence time in the furnace reactor or by additional post annealing processes. In morphology, dense and spherical particles showed much higher PL intensity than hollow, porous, and irregular shaped particles.

Crystallization of phosphor particles is mainly governed by the reaction temperature and time during either particle formation or post heat treatment. Reaction temperature in spray pyrolysis reactor showed a strong dependency on particle crystallinity [5–7]. Park et al. [5] reported that crystallization of Y_2O_3:Eu particles starts above 600 °C and it gets higher crystallinity as the reaction temperature increases up to 1,200 °C, which in turn results increased PL intensity at higher temperature. However, when they annealed particles at 1,200 °C, the PL intensity is increased about 30%. Therefore, they suggested using higher reaction temperatures to get higher PL intensity without post heat treatment. On the other hand, for high temperature system, an alumina tube (>1,200 °C) was used instead of a quartz tube (<1,200 °C), so alumina compounds was detected in the final phosphor particles. Higher reaction temperature revealed impurity addition to phosphor particles, which possibly reduced the PL intensity [7]. It was, however, suggested that the lower crystallinity in vicinity of particle surface formed under higher temperature gradient at the exit of pyrolysis reactor could reduce the PL intensity even without the alumina compounds [6]. Therefore, an

annealing step is necessary to improve PL intensity because there is no big advantage using high temperature in producing Y_2O_3:Eu particles without post heat treatment.

A few studies on the post heat treatment of phosphor particles to improve the PL intensity were reported [8–10]. The PL intensity was generally increased after the heat treatment step, but there was no monotonic increase with increasing the treatment temperature because of particle aggregation problem. It thus needs optimum temperature for the post heat treatment to get the highest PL intensity after the heat treatment process [8]. However, the heat treatment process could lead hollow and porous structure of particles [9, 10], so the flame spray pyrolysis method was also tried by other researchers [11–14] to form dense spherical particles before post heat treatment steps.

In the flame spray pyrolysis, the flame temperature is usually considered higher than 2,000 °C, so denser particles can be formed by melting of the material than in common spray pyrolysis case. One drawback from the high temperature flame pyrolysis is the formation of monoclinic crystal structure (generally formed in solid state at temperatures above 1,700 °C), which can reduce the PL intensity of particles and change the location of the emission peak. Therefore, post heat treatment is needed to transform the monoclinic crystal to the cubic crystal that leads higher PL intensity, and the PL intensity of particles formed by the flame spray pyrolysis was enhanced about 20% compared to that by the common spray pyrolysis after the post heat treatment [11]. In order to obtain the cubic crystal structure without a heat treatment step, optimum flame temperature is required by controlling the fuel gas and oxidizing gas ratio. The cubic-crystallized particles were produced without post heat treatment, and the PL intensity variation was demonstrated for the europium contents from 3 to 14 mol % [12]. In addition to the flame spray pyrolysis using the conventional nebulizer, a nozzle was used to generate droplets. Cubic Y_2O_3:Eu nanoparticles (<30 nm) were prepared with the nozzle-type droplet generator directly without post-processing by flame spray pyrolysis of appropriate organometallic precursors by Camenzind et al [13]. They also examined the change in phase content with changing specific enthalpy by varying precursor feed rate and oxygen dispersion gas flow rate. Increasing specific enthalpy leads higher content of the cubic phase than the monoclinic phase, which results in the sharp PL intensity peak at 612 nm from the broad peak at 625 nm. Purwanto et al. reported a systematic study of the comparison between the nebulizer and the nozzle in generation of droplets for the flame spray pyrolysis [14]. They concluded that the use of a nebulizer was much more effective on generating particles with high PL intensity than the use of a nozzle type generator because the former had a better control in producing high crystallinity and good morphology (spherical, dense, and non-agglomerated) than the latter.

In addition, many efforts were given for the colloidal seed-assisted spray pyrolysis [15, 16] and the addition of flux materials [16–21] to increase the PL intensity of particles. Colloidal seed (Yttrium hydroxy carbonate sols) helps the formation of filled structure of phosphor particles and it promotes the crystallinity of the particles [15]. However, this method has inherently process complexity for large-scale production with an additional seed formation step, so it may not be a good way in commercial applications. Flux additives [16–21] having relatively low melting points compared to Y_2O_3:Eu were also examined to improve the PL intensity by reducing particle surface defects and by increasing particle crystallinity. In using metal carbonate fluxes [17], small increase in crystallinity was observed, but no much change in crystallinity was seen in metal chloride fluxes cases [18, 19]. Rather, both fluxes help minimizing surface defects and it increases the PL intensity even without increased crystallinity. Using fluxes has a disadvantage by forming irregular (shrunken spherical structure) shaped particles because of their melting process during the particle formation. Thus, colloidal seed method was additionally used with the fluxes in order to overcome irregular shaped particle morphology [16]. Many researches were done to increase the PL intensity of phosphor particles by keeping spherical morphology after post heat treatment in laboratory experiments, but hollow and porous morphologies were observed in large-scale production after annealing step. Therefore, polymeric precursors were added to the spray pyrolysis solution to reduce those problems.

Ethylene glycol [22–25] and polyethylene glycol [26, 27] with citric acid were used to achieve spherical and filled particle morphology. Esterification reaction between the glycol and the acid occurs during the pyrolysis inside sprayed-droplets, and the polymer chains formed from the esterification reaction act as seeds to form dense volume precipitates inside the droplets. The droplets evolve into dense and spherical particles from the spray pyrolysis reactor, and it further keeps their shapes after the post heat treatments. Morphology of particles with polymeric precursors can be a function of molecular weight of polyethylene glycol, and denser particles were made from higher molecular weight of polyethylene glycol [27]. In order to get a maximum PL intensity value, the optimum amount of the precursor ratio (glycol/acid) should be used in preparation of the spraying solution. Further effort of using flux material was given for particles made with polymeric precursors to improve the brightness of spherical shaped phosphor particles [25]. Use of the flux material showed not only improvement of the brightness of the particles (similar to commercial products) by enhancing crystallinity

with increasing crystallite sizes [24] but also change of the particle size from micrometer to nanometer scale by melting the flux material during the post heat treatment. However, the nanometer-sized particles came with the aggregate morphology, and they required a ball milling process additionally.

Gd_2O_3:Eu

Gd_2O_3:Eu phosphor is also a popular compound under being developed in the red color applications for display devices. Many articles were published on this material for the effects of reaction temperature [28], annealing temperature [29–32], colloidal solution [33, 34], flux additive [34–38], and polymeric precursors [34, 36–40]. Generally, the PL intensity increases with increasing reaction temperature as similar as Y_2O_3:Eu because the crystallinity of the particles are improved at high temperature. Gd_2O_3:Eu phosphor, however, showed different phase formation depending on the reaction temperatures, for example cubic phase at the temperature lower than 1,400 °C and monoclinic phase at 1,600 °C. In both Y_2O_3:Eu and Gd_2O_3:Eu cases, high reaction temperature results in the formation of monoclinic crystal structure (Y_2O_3:Eu at temperature above 2,000 °C in the flame spray pyrolysis, Gd_2O_3:Eu at 1,600 °C in conventional spray pyrolysis). Therefore, it is desired to find the optimum reaction temperature to achieve the highest PL intensity.

Several studies [29–31] for investigations of crystal phases from the Gd_2O_3:Eu particles as prepared and annealed were reported. As prepared Gd_2O_3:Eu particle showed two types of cubic phases: space groups Ia3 and Fm3m. The Fm3m phase was disappeared after annealing at temperatures above 400 °C. This phase change after annealing affects the luminescence property because of the change of the crystal symmetry around the activator. After annealing, the sharp emission peak was only appeared at 612 nm due to the single cubic Gd_2O_3 phase (Ia3) which has C_2 symmetry site, whereas two dominant peaks were appeared at 615 nm and 624 nm from the as prepared Gd_2O_3:Eu particles. In addition, Wang et al. [32] observed locally formed monoclinic phase after annealing at 1,100 °C for 12 h with electron diffraction, which might result in broadened emission peak due to Eu^{3+} in a locally disordered gadolinium oxide matrix.

Colloidal solution (gadolinium hydroxycarbonate sol) approach was tried to achieve dense and spherical particle morphology for better packaging efficiency for film manufacturing, but the PL intensity was not changed much [33]. When the silica colloidal solution was used, cubic crystal structure was formed around 1,600 °C, but monoclinic crystal was the major without the silica colloidal solution [34]. Thus, the PL intensity is drastically increased because of the cubic crystal formation.

In addition to the flux materials used in Y_2O_3:Eu, boric acid (H_3BO_3) was studied for a flux additive to reduce particle surface defects. Crystallite size was increased when the boric acid was used as the flux additive, and the PL intensity was also increased with the proper amount of the boric acid [35]. In case of using polymeric precursor with flux materials (lithium carbonate, sodium carbonate, potassium carbonate, and lithium chloride), broken particle morphology was observed after the heat treatment. However, boric acid flux kept the spherical morphology after the heat treatment step. Therefore, boric acid flux can be recommended for use to keep spherical morphology from the thermal treatment [38].

$(Y,Gd)_2O_3$:Eu

Y_2O_3:Eu and Gd_2O_3:Eu described above are sometimes used as composite forms to improve its optical properties. The higher PL intensity was achieved from the composite particles in the Gd rich composition, and it was slightly higher than that from the Gd only particles. However, hollow and porous particle structure was the major challenge to overcome in the Gd rich composite particles. Thus, colloidal solution (gadolinium hydroxycarbonate sol) was introduced to make the hollow and porous structure into dense and spherical particles. As a result, the PL intensity of the particles produced with colloidal solution was slightly increased [41]. Sodium carbonate flux additive was used for the composite particles to reduce surface defects and to increase crystallite size, and the PL intensity was increased as expected [42]. Lithium chloride flux was also studied for the flame spray pyrolysis [43], which is applied for the dense particle production. It was effective to obtain high PL intensity at low post treatment temperature regardless of the composition ratio of Y/Gd. In addition, the required post treatment temperature to form cubic phase crystal was reduced as the ratio of Y/Gd increased no matter the flux. Polymeric precursor was also used for large-scale application of the composite particles to improve the particle morphology, and the similar results were shown with the yttrium and gadolinium cases [44]. In the aspect of the PL intensity, the composite particle case showed lower value than that of the Gd only particle case.

$(Y,Gd)BO_3$:Eu

It is widely used as red-emitting phosphor in plasma display panels (PDP) because of high luminescence efficiency under vacuum ultraviolet (VUV) excitation. Joffin et al. [45] produced Y_2O_3:Eu and YBO_3:Eu phosphor particles

with the same reaction condition, and they measured the PL intensity under VUV condition. They observed three splitted peaks in the emission spectra from the YBO_3:Eu phosphor particles, and the integrated Eu^{3+} emission intensity was about 50% higher than that from the Y_2O_3:Eu phosphor particles. However, it is very hard to control the particle morphology because of the low melting point and high volatility of the borate compounds. Kang and Park [46] used the reaction temperatures lower than 1,300 °C to achieve the maximum PL intensity of (Y,Gd)BO_3:Eu particles without forming amorphous structure, and they further used post annealing steps to enhance crystallinity. They also used Y or Gd hydroxy carbonate sol solutions to have filled and non-aggregated structures, and the PL intensity was increased about 45% with good particle morphology.

Kim and Lee [47] produced (Y,Gd)BO_3:Eu particles by both spray pyrolysis and solid-state reaction, and the results were compared. Uniform particle size distribution and spherical morphology were observed from the particles produced by spray pyrolysis, but hollow particle morphology was also formed by spray pyrolysis. In addition, the PL intensity of particles produced by spray pyrolysis was lower than that from solid-state reaction. A few studies [48–50] used polymeric precursors to reduce hollowness of phosphor particles, and which result in the improved PL intensity and dense-spherical particles at the optimum ratio of citric acid and ethylene glycol and at the optimum reaction temperature. Several co-dopants were studied to improve the PL intensity of (Y,Gd)BO_3:Eu particles [51], and the only indium (In) showed improved PL intensity compared to the commercial products.

Miscellaneous

In addition to the major red phosphor materials (europium-doped yttrium or gadolinium compounds) reviewed above, several other red phosphors were investigated by applying polymeric precursor [52–54], colloidal solution [55, 56], flux-additive [57–59], flame-spray pyrolysis [59, 60] approaches. Citric acid and polyethylene glycol as polymeric precursors were used for the preparation of YAG:Eu [52], YVO_4:Eu [53], and ZrO_2:Eu [54]. The particle morphology and the PL intensity were improved as demonstrated for the europium-doped yttrium or gadolinium compounds. However, there was no relative comparison of the performance for the PL intensities between the different compounds. Colloidal solution methods were used to improve particle morphology. Nano-silica colloidal solution was used to form spherical SiO_2:Eu particles [55]. Silica particles were utilized not only as colloidal seeds but also for the final host material in red phosphor. Ammonia was also used as an intermediate to help the formation of colloidal solution for (Y,Gd)$Al_3(BO_3)_4$:Eu particles [56], and high PL intensity was observed at the high gadolinium content. The red color purity of the borate compounds, (Y,Gd)BO_3:Eu, was also enhanced by adding aluminum component. $LiNO_3$ flux material was added for $SrTiO_3$:Pr,Al particle generation by the one-step spray pyrolysis [57] and by the flame spray pyrolysis [59]. Both studies showed the improved PL intensity. The flame spray pyrolysis approach was used to produce dense $SrTiO_3$:Pr,Al particles without post heat treatment process [59, 60], and those particles showed high PL intensity.

In the beginning of the spray pyrolysis researches for the generation of phosphor particles, a filter expansion aerosol generator (FEAG) was applied for $CaTiO_3$:Pr [61] and YAG:Eu [62]. Later, most studies used an ultrasonic nebulizer to produce precursor droplets.

Table 1 summarizes the results of major emission peaks from the various red phosphor particles.

Green phosphor

Zn_2SiO_4:Mn

Particle crystallinity and morphology are the major parameters to yield high PL intensity in phosphor materials, as

Table 1 Summary of emission peaks for the various red phosphor particles

Composition	Emission peak (nm)	References
Y_2O_3:Eu[a]	611	[5–27]
Gd_2O_3:Eu[b]	611	[28–40]
$(Y,Gd)_2O_3$:Eu[c]	611	[41–44]
(Y,Gd)BO_3:Eu[d]	593, 610, 625	[45–51]
YAG:Eu[e]	591*, 595, 608, 629	[52, 62]
YVO_4:Eu	593, 614, 618*	[53]
ZrO_2:Eu	591, 605*	[54]
SiO_2:Eu	590, 616*, 650, 700	[55]
(Y,Gd)$Al_3(BO_3)_4$:Eu	591, 595, 612*, 617, 627	[56]
$SrTiO_3$:(Pr,Al)	580–650, 620*	[57, 59, 60]
$Y(P,V)O_4$:Eu	580, 620*, 700	[58]
$CaTiO_3$:Pr	615	[61]

* Major peak

[a] Mostly cubic phase after annealing process. Broad and low intensity peak is appeared at 625 nm if monoclinic phase

[b] Mostly cubic phase after annealing process. Much similar emission spectrum with Y_2O_3:Eu is appeared. Low intensity peaks are appeared at 615, 624 nm if monoclinic phase

[c] Much similar emission spectrum with Y_2O_3:Eu

[d] Three strong emission peaks are appeared in the red-orange region and low color purity

[e] Single peak is appeared at 614 nm if FEAG used

demonstrated in red phosphors. Amongst many green phosphors, Zn_2SiO_4:Mn is most widely used in commercial PDP applications because of its high luminescent characteristics and chemical stability under vacuum ultraviolet light excitation. The FEAG process [63] was used to produce Zn_2SiO_4:Mn phosphor particles with spherical shape, nonaggregation, and submicron size after post heat treatment, and the green emission peak was observed at 527 nm. One-step synthesis for Zn_2SiO_4:Mn particles of 0.3–1.3 μm in size with spherical morphology and non-aggregation was reported [64], and the optimum temperature to form the highest crystallinity was found at 1,300 °C. When reaction temperature was higher than 1,400 °C, it was difficult to form crystal structure because of the high evaporation rate of Zn.

Citric acid additive was introduced to control morphology of phosphor particles by forming polymeric network during pyrolysis [65, 66]. In red phosphor cases, ethylene glycol was simultaneously used with citric acid to form polymeric precursor, but only citric acid was used in Zn_2SiO_4:Mn particles. Spherical, dense, non-aggregation characteristics were achieved using citric acid additive in spray pyrolysis, and higher PL intensity than commercial products was observed [65]. In film formation process, high density and uniformity of the packaging layer was demonstrated from the spherical Zn_2SiO_4:Mn particles generated with the citric acid approach [66].

Although the Zn_2SiO_4:Mn material has the high luminescent property, it has a drawback of long decay time compared to the commercial products. Generally, the higher Mn content reduces the decay time, and the Mn content affects the PL intensity as well as the decay time. The Mn content was varied from 5 to 12 mol % [67], and the PL intensity was the highest at 5 mol % with the longest decay time. In order to find the optimum condition for the high PL intensity and short decay time, post annealing temperature was also tested. At 10 mol % of Mn and at 1,155 °C annealing temperature, the PL intensity was increased at the similar level of the decay time with the commercial product. The addition of proper amount of barium (Ba) co-dopant also showed short decay time and higher PL intensity than the commercial phosphor [68].

(Ce,Tb)$MgAl_{11}O_{19}$

Several articles were published on this material. Excitation energy is transferred from Ce^{3+} to Tb^{3+} in this compound, and a green luminescent peak appears. Spherical amorphous micron particles were produced at temperatures lower than 900 °C, and they were annealed to form crystalline structure at temperatures higher than 1,200 °C [69]. Phase pure crystal was obtained after annealed at temperature above 1,400 °C, but particles had aggregate and irregular morphology. Therefore, one-step spray pyrolysis at 1,500 °C was used to form spherical-shaped particles, and the PL intensity was found to be similar level with particles annealed. Thus, one-step approach was further studied at higher temperature than 1,500 °C to increase the PL intensity with increasing crystallinity by keeping spherical particle morphology [70]. As a result, the PL intensity and crystallinity of particles were higher than those from annealed particles.

Boric acid flux was introduced to enhance particle morphology and the PL intensity. The PL intensity was increased after post heat treatment with increasing crystallinity [71], and the particle morphology still had irregular and aggregate shapes with addition of the boric acid flux. However, particle morphology produced by the one-step pyrolysis with the proper amount of the boric acid flux was spherical, and the PL intensity was higher than those without the flux [72]. In addition, various types of flux additives (NH_4Cl, LiCl, H_3BO_3, Li_2CO_3, $NH_4H_2PO_4$) were used to examine the brightness of phosphor particles with spherical shape and filled morphology [73]. The H_3BO_3 and $NH_4H_2PO_4$ fluxes showed the best performance for the PL intensity and particle morphology without post heat treatment process.

Polymeric precursors (citric acid and ethylene glycol) were used to keep spherical particle morphology after post heat treatment [74]. As expected, dense, spherical, and non-aggregate morphologies were seen, but the PL intensity was turned out to be similar as particles generated without the polymeric precursors.

Y_2SiO_5:Tb

This compound is also green-emitting phosphor and a few articles were published on this material. Effects of the reaction and annealing temperatures on the crystallinity were reported [75]. Particle crystallinity was increased with increasing reaction temperature (800–1,200 °C) and annealing temperature (900–1,200 °C), and it resulted in high PL intensity. However, the annealing temperature of 1,400 °C did not show improvement of the PL intensity, and the monoclinic crystal phase was transformed from X-1 type to X-2 type. When fumed silica particles (14 nm) were used as a silicon source for the colloidal solution [76], and the crystal phase transformation from X-1 type to X-2 type was also observed at the annealing temperature above 1,200 °C. The Y_2SiO_5:Tb phosphor particles with complete X-2 type crystal structure had higher PL intensities than those with X-1 type crystal structure. The excess amount of stoichiometric fumed silica particles showed high crystallinity of X-2 type and high photoluminescent intensity. A study on the preparation methods of particles from colloidal solution and

aqueous solution was performed [77]. The particles prepared from the colloidal solution with fumed silica particles had a pure monoclinic X-2 phase after annealing at 1,300 °C. On the other hand, the particles prepared from tetraethyl orthosilicate (TEOS) reagent had X-2 phase with small amount of X-1 phase due to the phase-segregation characteristics of the TEOS precursor. The PL intensity of Y_2SiO_5:Tb particles were strongly affected by the silicon source used.

One-step spray pyrolysis can be used to produce Y_2SiO_5:Tb particles since the PL intensity of as-prepared particles at 1,200 °C was much similar level to the maximum intensity of calcined particles [75]. One-step method was applied for the generation of Y_2SiO_5:Tb particles at high temperature (>1,200 °C) [78]. The particles produced at 1,650 °C showed higher PL intensity than that of calcined particles, and the crystal structure was X-1 type. NH_4F flux additive was introduced to improve the PL intensity, and the higher brightness was shown from the Y_2SiO_5:Tb particles. Lee et al. [78] also suggested that material crystallinity and its phase purity can be considered as the major parameters regardless of the crystal structure (X-1 type or X-2 type) for the high PL intensity.

YAG:(Ce or Tb)

YAG is used as the host material for all color phosphors by changing the dopants such as Ce, Tb, Eu, and Tm. Among the dopants, Ce and Tb generate green light in the YAG host material. YAG:Ce particles were produced by the FEAG process [79] and by the ultrasonic nebulizer [79–81]. The annealing temperature to obtain high crystallinity with those processes was much lower than that with the conventional solid-state process. The PL intensity of the YAG:Ce particles was governed by the Ce concentration, annealing temperature, mean particle size, and particle morphology. YAG:Tb particles were also produced by the ultrasonic spray pyrolysis [82]. Particle crystallinity after the annealing step was higher than that from the commercial products, and particle sphericity was kept with non-aggregation characteristics. However, the PL intensity was not improved to the commercial products from the solid-state process. It might come from the particle porosity. In order to examine the possibility of the large-scale production, polymeric precursor approach was used to reduce hollowness and porosity [83, 84]. In addition to the polymeric precursor, the flux additive was also used to improve the PL intensity [84]. As a result, spherical and dense particles were obtained through volumetric precipitation inside droplets and thus the PL intensity was increased.

Miscellaneous

Many other types of multi-component oxide particles for green phosphor materials were reported. Especially, efforts were given to replace Zn_2SiO_4:Mn phosphors for display device applications with various compounds: $BaAl_{12}O_{19}$:Mn [85, 86], $GdPO_4$:Tb [87, 88], $GdPO_4$:(Tb,Mn) [89], $LaPO_4$:(Tb,Mn) [89], $ZnGa_2O_4$:Mn [90], YBO_3:Tb [91] particles. In addition to the display device applications, several green phosphors were developed for the applications of the fluorescent lamp and the ultraviolet light emitting diode (UV LED). For the fluorescent lamp applications, $LaPO_4$:(Ce,Tb) [92, 93] and YVO_4:Dy [94] particles were investigated. Much complicated chemical compositions such as $(Ba,Sr)_2SiO_4$:Eu [95], $Ca_8Mg(SiO_4)_4Cl_2$:Eu [96], and $(Sr,Zn)Al_2O_4$:Eu,B [97] particles were used to produce green phosphor materials for the UV LED applications.

As expected, particles produced from the spray pyrolysis process showed spherical and non-aggregate morphology under optimum preparation conditions, compared to the products from the solid-state reaction. The PL intensity could be improved by various approaches such as change of the reaction temperature, post heat treatment, use of the colloidal solution, and use of the polymeric precursor.

Table 2 summarizes the results of major emission peaks from the various green phosphor particles.

Blue phosphor

$BaMgAl_{10}O_{17}$:Eu

This is a typical blue phosphor material for PDP applications because of its high luminescence characteristics under vacuum ultraviolet excitation. Commercial phosphor particles from the solid-state process have irregular-shaped morphology, and it reduces the packing density and uniformity of the film. Therefore, spray pyrolysis method has been deployed in production of the $BaMgAl_{10}O_{17}$:Eu particles to achieve spherical particle morphology. Kang et al. [98] reported morphological variations of multi-component oxide phosphor particles by high temperature spray pyrolysis. High sphericity and non-aggregate property were obtained at high reaction temperature, but those morphological properties were significantly disappeared after post heat treatment. The PL intensity of the particles without the post heat treatment was higher than that with. However, it was still much lower than the PL intensity from the commercial products. Thus, another approach to achieve high PL intensity of the particles produced without annealing process was studied, addition of flux material for example.

Table 2 Summary of emission peaks for the various green phosphor particles

Composition	Emission peak (nm)	References
Zn_2SiO_4:Mn[a]	475–625, 525*	[63–68]
(Ce,Tb)$MgAl_{11}O_{19}$	486, 545*, 585, 624	[69–74]
Y_2SiO_5:Tb[b]	484, 538*, 585, 624	[75–78]
YAG:Ce[c]	480–650, 528*	[79–81]
YAG:Tb	490, 544*, 585, 592, 625	[82–84]
$BaAl_{12}O_{19}$:Mn	475–600, 516*	[85, 86]
$GdPO_4$:Tb	480, 547*, 580, 620	[87, 88]
$LaPO_4$:(Tb,Mn)	480, 547*, 580, 620	[89]
$ZnGa_2O_4$:Mn	475–550, 500*	[90]
YBO_3:Tb	488, 540*, 587, 625	[91]
$LaPO_4$:(Ce,Tb)	487, 543*, 582	[92, 93]
YVO_4:Dy	483, 574*	[94]
$(Ba,Sr)_2SiO_4$:Eu	460–580, 508*	[95]
$Ca_8Mg(SiO_4)_4Cl_2$:Eu	460–550, 502*	[96]
(Sr,Zn)Al_2O_4:Eu,B	450–600, 520*	[97]

* Major peak

[a] Broad emission spectrum. Peak is shifted to longer wavelength with increasing dopant concentration

[b] Crystal phase transition is accompanied from X-1 to X-2 by annealing process

[c] Broad emission spectrum

Ammonium chloride (NH_4Cl) flux was introduced to the precursor solution [99], but the PL intensity (higher than without the flux) was still lower than that of the commercial products. Possible reason of the low PL intensity could be from the presence of water vapor which prevents the formation of reducing atmosphere inside the furnace reactor. Other researchers showed results on the reducing conditions to improve the PL intensity of the blue phosphors. Jeon et al. [100] prepared spherical $BaMgAl_{10}O_{17}$:Eu particles by spray pyrolysis technique, and they annealed the particles under reducing atmosphere (95% N_2 + 5% H_2) in various temperatures (1,000–1,600 °C). The high PL intensity was achieved from the particles annealed at 1,600 °C, and it showed the similar level with the commercial products. Therefore, reducing process may be required to achieve high PL intensity in $BaMgAl_{10}O_{17}$:Eu phosphors since it is difficult to activate the Eu component through one step production.

Various precursor types such as nitrate, hydroxide, acetate, and chloride were tested in spray pyrolysis to examine their effects on particle morphology and the PL intensity [101]. Amongst those metallic precursors, the optimum combination of barium-magnesium-aluminum precursors for high brightness and spherical morphology was the nitrate-nitrate-nitrate. Other combinations including chloride precursors showed non-spherical morphology and poor photoluminescence characteristics.

In addition, several studies on improving particle morphology and PL intensity were carried out with colloidal solution, aluminum metal, aluminum polycation, and polymeric precursors (citric acid and polyethylene glycol). Aluminum isopropoxide was used to make the colloidal solution [102], and it helped forming spherical particles with nonaggregation characteristics after post heat treatment. Aluminum metal bits associated with aluminum nitrate non-hydrate were dissolved in distilled water to increase solution viscosity [103], and it resulted in dense particle morphology due to the reduction of decomposed nitrate group in each droplet. The PL intensity of the particles with aluminum metal bits in the precursor solution was improved and it was higher than that of commercial products. In aluminum polycation approaches [104–106], the aluminum nitrate precursor solution was chemically modified with NH_4OH. It also showed good spherical morphology after annealing process and high PL intensity. Further improvement of the PL intensity in the polycation method was achieved with additional co-dopants (Er and Nd) [105]. As reviewed in red phosphor particles, polymeric precursors (citric acid and polyethylene glycol) were used in blue phosphors to get good morphology and high PL intensity [107]. Molecular weight of the polyethylene glycols and the amount of the organic additives were the major parameters in preparation of particles having good morphology and high PL intensity.

Flame spray pyrolysis method was also tried for this phosphor material [108, 109]. Dense and spherical particles were obtained by the flame spray pyrolysis, and those particles were used to form phosphor films. The PL intensity from the film manufactured with the spherical particles was higher than that with commercial irregular ones [108]. Great attention needs to be paid in blue phosphor particles because annealing process is necessary to activate Eu in host materials under reduction atmosphere.

There was a study on the thermal degradation of $BaMgAl_{10}O_{17}$:Eu phosphors [110]. The remaining oxygen source, for example water, interacts with the activator Eu^{2+} and changes its valence. Therefore, the thermal degradation of the phosphor materials is occurred, and the color

properties (emission intensity and purity) were changed. A two-step post-thermal treatment was used: (i) 400 °C under vacuum atmosphere and (ii) 1,400 °C under reducing atmosphere. As a result, thermal degradation was minimized by forming a stable hydrophobic surface which was maintained even after film making process, and color shift was effectively prevented.

Miscellaneous

Sr_2CeO_4 material was studied to explore additional blue phosphor for applications to the fluorescent lamp by incorporating with flux additive and polymeric precursors. NH_4NO_3 flux addition in preparation of the Sr_2CeO_4 phosphor showed finely distributed spherical and non-aggregate particle morphology after heat treatments at temperatures below 1,000 °C for 2 h [111]. Polymeric precursors of a citric acid with ethylene glycol [112] or polyethylene glycol [113] were used for generation of Sr_2CeO_4 particles. Particle morphology revealed non-spherical shape with the use of ethylene glycol although the PL intensity was increased. However, it was improved with the polyethylene glycol. The use of polymeric precursor approaches might need additional milling process because Sr_2CeO_4 particles still had aggregate and not-quite spherical shaped morphology. The $Sr_5(PO_4)_3Cl$:Eu phosphor particles were also investigated using the conventional spray pyrolysis [114] and the flame spray pyrolysis [115] methods. Various types of precursor sources were used in the conventional spray pyrolysis. Phase pure halophosphate spherical non-aggregated particles were obtained using the ammonium phosphate and ammonium dihydrogen phosphate as phosphorous sources. Strontium nitrate and strontium chloride mixture were used as the strontium and chlorine sources for the best morphological performance. The above chemical combination showed the highest PL intensity from the particles generated by the conventional spray pyrolysis. The PL intensity of particles produced by the flame spray pyrolysis was much more enhanced than those by the conventional spray pyrolysis after heat-treatments with NH_4Cl flux. This might be due to the large crystallite size in particles from the flame spray pyrolysis. The Y_2SiO_5:Ce phosphor particles 0.5–1.4 μm in size were prepared with spherical morphology [116]. Crystal structure of the material was shifted from X-1 to X-2 at annealing temperatures above 1,200 °C, and thus slight color shift was also accompanied. Higher PL intensity than the commercial products was achieved at the annealing temperatures above 1,400 °C. Jung et al. [117] prepared $CaMgSi_2O_6$:Eu phosphor particles to examine the thermal stability. The color shift was not observed after the film making process, and the reduction of the emission intensity was small compared to the case with $BaMgAl_{10}O_{17}$:Eu particles. In addition, the maximum PL intensity of the $CaMgSi_2O_6$:Eu particles was very similar to that of the $BaMgAl_{10}O_{17}$:Eu particles. Therefore, the $CaMgSi_2O_6$:Eu particles could be used as an alternative blue phosphors for the next generation of PDP.

Table 3 summarizes the results of major emission peaks from the various blue phosphor particles.

Table 3 Summary of emission peaks for the various blue phosphor particles

Composition	Emission peak (nm)	References
$BaMgAl_{10}O_{17}$:Eu[a]	400–525, 450*	[98–110]
Sr_2CeO_4[b]	400–650	[111–113]
$Sr_5(PO_4)_3Cl$:Eu[c]	375–500, 446*	[114, 115]
Y_2SiO_5:Ce[d]	375–550	[116]
$CaMgSi_2O_6$:Eu[e]	400–525, 447*	[117]

* Major peak

[a] Peak is shifted to longer wavelength region with low intensity after film making process

[b] Major peaks are appeared at 455, 467, and 470 nm depending on additives

[c] Broad maximum at 446 nm

[d] Broad peak is shown with the similar intensity at 400 nm and 450 nm. Single peak is appeared with low annealing temperature, whereas two peaks with high annealing temperature(>1,300 °C)

[e] Broad emission spectrum

Summary

Red, green, and blue phosphor particles prepared by spray pyrolysis were intensively reviewed. Each phosphor has its own emission peak as summarized in Table 1, 2, and 3. Particle morphology from the spray pyrolysis is highly spherical because every spherical droplet evolves into final particle through a high temperature furnace, where solvent is evaporated and precursors are decomposed. However, particles can have hollow and porous structures because of the abrupt change of reaction temperature as well as relatively short reaction time in the furnace reactor. Thus, several additional approaches such as the use of colloidal solutions, flux materials, polymeric precursors, and flame spray pyrolysis were studied to overcome the morphological problems. Those efforts showed improved results in morphology, which in turn increased the PL intensity of particles. The PL intensity is strongly affected by the material crystallinity and phase purity. Many efforts were given to increase the PL intensity of particles produced by high reaction temperature or additional heat treatments. Generally, high temperature favors in formation of high crystallinity, but it could result in high aggregation morphology which leads low PL intensity. Spherical phosphor

particles having high crystallinity and phase purity generated by spray pyrolysis are expected to produce high packaging density and uniformity for film applications of flat panel display devices. Therefore, spray pyrolysis method is considered as a successful candidate for the production of phosphor particles in large scale applications, compared with the conventional solid-state process.

References

1. Shionoya S, Yen WM (1999) Phosphor handbook. CRC Press, New York
2. Ball DW (2003) Physical chemistry. Brooks/Cole-Thomson Learning, Singapore
3. Rack PD, Holloway PH (1998) Mater Sci Eng R21:171
4. Atkins PW (1998) Physical chemistry. Oxford University Press, Oxford
5. Park SB, Kang YC, Lenggoro IW, Okuyama K (1998) J Aerosol Sci 29:S909
6. Shimomura Y, Kijima N (2004) Electrochemical and Solid-State Letters 7:H18
7. Shimomura Y, Kijima N (2004) Electrochemical and Solid-State Letters 7:H1
8. Hong GY, Jeon BS, Yoo YK, Yoo JS (2001) Journal of The Electrochemical Society 148:H161
9. Joffin N, Caillier B, Dexpert-Ghys J, Verelst M, Baret G, Garcia A, Guillot P, Galy J, Mauricot R, Schamm S (2005) J Phys D: Appl Phys 38:3261
10. Joffin N, Dexpert-Ghys J, Verelst M, Baret G, Garcia A (2005) J Luminescence 113:249
11. Kang YC, Seo DJ, Park SB, Park HD (2001) Jpn J Appl Phys 40:4083
12. Chang H, Lenggoro IW, Okuyama K, Kim T-O (2004) Jpn J Appl Phys 43:3535
13. Camenzind A, Strobel R, Pratsinis SE (2005) Chem Phys Lett 415:193
14. Purwanto A, Leggoro IW, Chang H, Okuyama K (2006) J Chem Eng Jpn 39:68
15. Kang YC, Roh HS, Park SB (2000) Adv Mater 12:451
16. Kang YC, Roh HS, Park SB, Park HD (2002) J Mater Sci Lett 21:1027
17. Kang YC, Roh HS, Seo DJ, Park SB (2000) J Mater Sci Lett 19:1225
18. Kang YC, Park HD, Park SB (2000) Jpn J Appl Phys 39:L1305
19. Kang YC, Roh HS, Park SB, Park HD (2002) J Eur Ceram Soc 22:1661
20. Hong GY, Yoo K, Moon SJ, Yoo JS (2003) J Electrochem Soc 150:H67
21. Shimomura Y, Kijima N (2004) J Electrochem Soc 151:H86
22. Sohn JR, Kang YC, Park HD (2002) Jpn J Appl Phys 41:3006
23. Jung KY, Han KH (2005) Electrochem Solid-State Lett 8:H17
24. Jung KY, Lee CH, Kang YC (2005) Mater Lett 59:2451
25. Lee CH, Jung KY, Choi JG, Kang YC (2005) Mater Sci Eng B 116:59
26. Roh HS, Kang YC, Park HD, Park SB (2003) Appl Phys A 76:241
27. Wang LS, Zhou YH, Quan ZW, Lin J (2005) Mater Lett 59:1130
28. Kang YC, Park SB, Lenggoro IW, Okuyama K (1999) J Phys Chem Solids 60:379
29. Milosevic O, Mancic L, Jordovic B, Maric R, Ohara S, Fukui T (2003) J Mater Processing Technol 143–144:501
30. Milosevic O, Mancic L, Rabanal ME, Torralba JM, Yang B, Townsend P (2005) J Electrochem Soc 152:G707
31. Rabanal ME, Moral C, Torralba JM, Mancic L, Milosevic O (2005) J Eur Ceram Soc 25:2023
32. Wang Y, Milosevic O, Gomez L, Rabanal ME, Torralba JM, Yang B, Townsend P (2006) J Phys: Condens Matter 18:9257
33. Kang YC, Roh HS, Park SB (2000) J Electrochem Soc 147:1601
34. Koo HY, Ju SH, Jung DS, Hong SK, Kim DY, Kang YC (2006) Jpn J Appl Phys 45:5018
35. Kang YC, Roh HS, Park SB (2000) Jpn J Appl Phys 39:L31
36. Kang YC, Roh HS, Kim EJ, Park SB (2003) J Electrochem Soc 150:H93
37. Roh HS, Kim EJ, Kang HS, Kang YC, Park HD, Park SB (2003) Jpn J Appl Phys 42:2741
38. Jung DS, Hong SK, Lee HJ, Kang YC (2006) Opt Mater 28:530
39. Lim MA, Kang YC, Park HD (2001) J Electrochem Soc 148:H171
40. Kang YC, Roh HS, Park SB, Jung KY (2004) Jpn J Appl Phys 43:5302
41. Roh HS, Kang YC, Park SB (2000) J Colloid Interface Sci 228:195
42. Kang YC, Roh HS, Park SB (2001) J Am Ceram Soc 84:447
43. Seo DJ, Kang YC, Park SB (2003) Appl Phys A 77:659
44. Kim EJ, Kang YC, Park HD, Ryu SK (2003) Mater Res Bull 38:515
45. Joffin N, Caillier B, Garcia A, Guillot P, Galy J, Fernandes A, Mauricot R, Dexpert-Ghys J (2006) Opt Mater 28:597
46. Kang YC, Park SB (1999) Jpn J Appl Phys 38:L1541
47. Kim D-S, Lee R-Y (2000) J Mater Sci 35:4777
48. Sohn JR, Kang YC, Park HD, Yoon SG (2002) Jpn J Appl Phys 41:6007
49. Jeoung BW, Hong GY, Yoo WT, Yoo JS (2004) J Electrochem Soc 151:H213
50. Koo HY, Jung DS, Ju SH, Hong GY, Kang YC (2006) Mater Lett 60:3091
51. Jung KY, Kim EJ, Kang YC (2005) J Ind Eng Chem 11:280
52. Zhou YH, Lin J, Yu M, Han SM, Wang SB, Zhang HJ (2003) Mater Res Bull 38:1289
53. Zhou YH, Lin J (2005) Opt Mater 27:1426
54. Quan ZW, Wang LS, Lin J (2005) Mater Res Bull 40:810
55. Jokanovic V, Dramicanin MD, Andric Z (2006) Acta Chim Slov 53:23
56. Wang LS, Liu XM, Quan ZW, Kong DY, Yang J, Lin J (2007) J Luminescence 122–123:36
57. Lenggoro IW, Panatarani C, Okuyama K (2004) Mater Sci Eng B 113:60
58. Shimomura Y, Kurushima T, Olivia R, Kijima N (2005) Jpn J Appl Phys 44:1356
59. Chang H, Lenggoro IW, Okuyama K, Jang HD (2006) Jpn J Appl Phys 45:967
60. Kang YC, Seo DJ, Park SB, Park HD (2002) Mater Res Bull 37:263
61. Kang YC, Choi JS, Park SB, Cho HS, Yoo JS, Lee JD (1997) J Aerosol Sci 28:S541
62. Kang YC, Chung YS, Park SB (1999) J Am Ceram Soc 82:2056
63. Kang YC, Park SB (2000) Mater Res Bull 35:1143
64. Lenggoro IW, Iskandar F, Mizushima H, Xia B, Okuyama K, Kijima N (2000) Jpn J Appl Phys 39:L1051
65. Roh HS, Kang YC, Lee CH, Park HD, Park SB (2003) Jpn J Appl Phys 42:3429
66. Lee CH, Kang YC, Jung KY, Choi JG (2005) Mater Sci Eng B 117:210
67. Kang YC, Park HD (2003) Appl Phys A 77:529
68. Kang YC, Lim MA, Park HD, Han M (2003) J Electrochem Soc 150:H7

69. Kang YC, Park SB, Lenggoro IW, Okuyama K (1999) Jpn J Appl Phys 38:2013
70. Kang YC, Lenggoro IW, Park SB, Okuyama K (2001) Appl Phys A 72:103
71. Jung DS, Hong SK, Lee HJ, Kang YC (2005) J Alloys Compounds 398:309
72. Jung DS, Hong SK, Ju SH, Koo HY, Kang YC (2006) Jpn J Appl Phys 45:116
73. Hong SK, Jung DS, Ju SH, Koo HY, Kang YC (2006) J Mater Sci: Mater Electron 17:341
74. Jung DS, Hong SK, Ju SH, Lee HJ, Kang YC (2005) Jpn J Appl Phys 44:4975
75. Kang YC, Lenggoro IW, Okuyama K, Park SB (1999) J Electrochem Soc 146:1227
76. Kang H-S, Kang Y-C, Park H-D, Shul Y-G (2003) Korean J Chem Eng 20:930
77. Kang HS, Kang YC, Park HD, Shul YG (2005) Appl Phys A 80:347
78. Lee HJ, Hong SK, Jung DS, Ju SH, Koo HY, Kang YC (2006) Ceram Int 32:865
79. Kang YC, Park SB, Lenggoro IW, Okuyama K (1998) J Aerosol Sci 29:S911
80. Kang YC, Lenggoro IW, Park SB, Okuyama K (2000) Mater Res Bull 35:789
81. Rosario GD, Ohara S, Mancic L, Milosevic O (2004) Appl Surface Sci 238:469
82. Kang YC, Lenggoro IW, Park SB, Okuyama K (1999) J Phys Chem Solids 60:1855
83. Jung KY, Lee DY, Kang YC (2005) Mater Res Bull 40:2212
84. Lee HJ, Hong SK, Jung DS, Kang YC (2005) Mater Lett 59:2383
85. Kang YC, Chung YS, Park SB (1999) J Mater Sci Lett 18:779
86. Lee DY, Kang YC, Park HD, Ryu SK (2003) J Alloys Compounds 353:252
87. Lee KK, Kang YC, Jung KY, Park HD (2002) Electrochem Solid-State Lett 5:H31
88. Lee KK, Kang YC, Jung KY, Park HD (2002) Jpn J Appl Phys 41:5590
89. Jung KY, Lee KK, Kang YC, Park HD (2003) J Mater Sci Lett 22:1527
90. Roh HS, Kang YC, Park SB, Park HD (2002) Jpn J Appl Phys 41:4559
91. Jung KY, Kim EJ, Kang YC (2004) J Electrochem Soc 151:H69
92. Lenggoro IW, Xia B, Mizushima H, Okuyama K, Kijima N (2001) Mater Lett 50:92
93. Kang YC, Kim EJ, Lee DY, Park HD (2002) J Alloys Compounds 347:266
94. Zhou YH, Lin J (2006) J Alloys Compounds 408–412:856
95. Kang HS, Hong SK, Kang YC, Jung KY, Shul YG, Park SB (2005) J Alloys Compounds 402:246
96. Kang HS, Hong SK, Koo HY, Ju SH, Kang YC, Jung KY, Park SB (2006) Jpn J Appl Phys 45:1617
97. Jung KY, Lee HW, Jung H-K (2006) Chem Mater 18:2249
98. Kang YC, Park SB, Lenggoro IW, Okuyama K (1999) J Electrochem Soc 146:2744
99. Shimomura Y, Kijima N (2004) J Electrochem Soc 151:H192
100. Jeon BS, Hong GY, Yoo YK, Yoo JS (2001) J Electrochem Soc 148:H128
101. Kang YC, Roh HS, Park HD, Park SB (2003) Ceram Int 29:41
102. Kang YC, Park SB (2000) J Electrochem Soc 147:799
103. Jung H-K, Lee D-W, Jung KY, Boo J-H (2005) J Alloys Compounds 390:189
104. Lee DY, Kang YC, Jung KY (2003) Electrochemical and Solid-State Letters 6:H27
105. Jung KY, Lee DY, Kang YC, Park HD (2003) J Luminescence 105:127
106. Jung KY, Lee DY, Kang YC, Park SB (2004) Korean J Chem Eng 21:1072
107. Zhou Y, Lin J (2005) J Solid State Chem 178:441
108. Jung KY, Kang YC (2004) Mater Lett 58:2161
109. Chang H, Lenggoro IW, Ogi T, Okuyama K (2005) Mater Lett 59:1183
110. Jung KY, Lee DY, Kang YC (2005) J Luminescence 115:91
111. Kang M-J, Choi S-Y (2002) J Mater Sci 37:2721
112. Hong SK, Ju SH, Koo HY, Jung DS, Kang YC (2006) Mater Lett 60:334
113. Liu X, Luo Y, Lin J (2006) J Crystal Growth 290:266
114. Lee JH, Kang YC, Park SB, Park HD (2001) Jpn J Appl Phys 40:3222
115. Kang YC, Sohn JR, Yoon HS, Jung KY, Park HD (2003) J Electrochem Soc 150:H38
116. Kang YC, Lenggoro IW, Park SB, Okuyama K (1999) J Solid State Chem 146:168
117. Jung KY, Han KH, Kang YC, Jung H-K (2006) Mater Chem Phys 98:330